

The Sentinel Margin: Intraoperative *Ex Vivo* Specimen Mapping Using Relative Fluorescence Intensity



Stan van Keulen^{1,2}, Naoki Nishio¹, Andrew Birkeland¹, Shayan Fakurnejad¹, Brock Martin³, Tim Forouzanfar², Kristen Cunanan⁴, A. Dimitrios Colevas⁵, Nynke S. van den Berg¹, and Eben Rosenthal¹

Abstract

Purpose: Despite major advancements in surgical oncology, the positive margin rate for primary head and neck cancer resection remains around 15%–30%. In particular, the deep surface margin is the most challenging to adequately assess. Inadequate margins are directly correlated to poor survival, and as such, mitigation of these rates is critical to improve patient outcomes. We have developed an *ex vivo* imaging strategy that utilizes fluorescence intensity peaks (relative to background signal) of an injected anti-EGFR antibody conjugated to a fluorescent probe to locate potential close or positive margins on the deep surface of the resected tumor specimen.

Experimental Design: Twelve patients with head and neck cancer scheduled for surgery received systemic administration of a tumor-specific contrast-agent (panitumumab-IRDye800CW). After surgical resection, the tumor specimen was imaged using a fluorescence imager. The three highest

fluorescence intensity-peaks on the deep surface of the specimen were isolated and correlated to histology to determine the margin distance at these regions.

Results: Relative fluorescence peak intensities identified the closest margin on the deep surface of the specimen within 2.5 minutes. The highest intensity peak consistently (100%) detected the closest margin to the tumor. The difference in tumor margin distance between the first and second highest fluorescence intensity peak averaged 2.1 ± 1.4 mm. The tumor-margin difference between the second and third highest peak averaged 1.6 ± 0.6 mm.

Conclusions: Fluorescence intensity peaks can identify the region on the specimen where tumor is closest to specimen's edge on the deep surface. This technique could have broad applications in obtaining adequate margins in oncological surgery.

Introduction

Surgical resection is the primary curative treatment for the majority of solid tumors. In the management of head and neck squamous cell carcinoma, resection of the primary tumor is considered adequate or clear when the surgical margins are >5 mm and inadequate if <5 mm, on final histology (1–3). Failure to obtain clear surgical margins is associated with locoregional recurrence and poor overall survival rates (4) and may necessitate additional therapy such as chemotherapy, radiotherapy, and/or

revision surgeries (5). Unfortunately, the highest overall inadequate margins rates (15%–30%) in all of surgical oncology are found in head and neck cancer (6). Despite the introduction of many novel technologies, inadequate margin rates have not changed over the past 30 years as surgeons cannot successfully differentiate healthy from diseased tissue (6, 7). The most commonly used method for intraoperative margin control is frozen section analysis (FSA); however, this technique suffers from sampling errors as surgeons often struggle to identify which suspicious regions should be sent for histopathologic assessment (8). This makes FSA not only a time-intensive technique (15–20 minutes/section), but also a subjective evaluation method (9).

After resection, the tumor specimen is anatomically divided into the peripheral surface (i.e., epithelial or mucosal surface) and the deep surface. The term deep surface describes the nonepithelial margin of the tumor specimen, which is exposed after surgical resection. In general, intraoperative margin assessment of the deep surface is more challenging compared with the visible and palpable peripheral margins (10). The lack of visual feedback makes the deep surface more at risk for having inadequate margins (11). This is illustrated by Woolgar and colleagues who evaluated 301 patients with oral cancer and showed that 87% of inadequate margins were located on the deep surface compared with 16% on the peripheral surface (1).

To address the challenges hindering effective intraoperative margin assessment (and in particular the deep margin), we propose a novel methodology for rapid and accurate

¹Department of Otolaryngology–Division of Head and Neck Surgery, Stanford University School of Medicine, Stanford, California. ²Department of Oral and Maxillofacial Surgery/Oral Pathology, VU University Medical Center/Academic Centre for Dentistry Amsterdam (ACTA), Amsterdam, the Netherlands. ³Department of Clinical Pathology, Stanford University School of Medicine, Stanford, California. ⁴Quantitative Sciences Unit, Stanford University School of Medicine, Stanford, California. ⁵Department of Medicine, Division of Medical Oncology, Stanford University School of Medicine, Stanford, California.

Note: Supplementary data for this article are available at Clinical Cancer Research Online (<http://clincancerres.aacrjournals.org/>).

Corresponding Author: Eben L. Rosenthal, Stanford University, 900 Blake Wilbur Drive, Stanford, CA 94305. Phone: 650-498-6000; Fax: 650-724-1458; E-mail: elr@stanford.edu

Clin Cancer Res 2019;25:4656–62

doi: 10.1158/1078-0432.CCR-19-0319

©2019 American Association for Cancer Research.

Translational Relevance

Surgical excision is an integral part of treatment for most solid tumors. An inadequate surgical margin occurs when cancer cells are near or present at the edge of the resected specimen. Inadequate margins correlate with a significantly worse survival and often warrant additional treatments, which result in patient morbidity and increase in health care cost. Despite new and costly operating room technologies and advanced training in surgical oncology, the rate at which patients leave the operating room with inadequate margins has not improved in the last three decades. Here, we present the results of a novel technique that enables surgeons to assess tumor at the deep surgical margin, which may be used to improve the rates of overall oncologically sound resections.

identification of the closest surgical margin on the specimen. We investigated real-time margin detection assessment using relative fluorescence intensity peaks after injection of a targeted fluorescent agent to identify positive and close margins (tumor < 5 mm). This methodology can assist the surgeon to take immediate corrective action during the procedure (12).

Materials and Methods

Study design

A phase I study evaluating panitumumab-IRDye800CW was approved by the Stanford Institutional Review Board (IRB-35064; NCT02415881) and the FDA (NCT02415881); written informed consent was obtained from all patients. The study was performed in accordance with the Declaration of Helsinki, FDA's ICH-GCP guidelines, and United States Common Rule. More details on the safety and pharmacokinetics of the phase I study can be found in Gao and colleagues (13). Briefly, consenting patients ($n = 16$) were infused 1–5 days prior to surgery with panitumumab-IRDye800CW [(excitation/emission max: 774/789 nm; dose: 25 mg/50 mg flat-dose; half-life: 24 hours (13)]. The dosing was not weight based: subjects received either a 25 mg ($n = 5$) or a 50 mg ($n = 11$) flat-dose of panitumumab-IRDye800CW. After resection, the deep surface of the tumor specimen was imaged using a closed-field fluorescence imaging device (PEARL, LI-COR Biosciences) before being sent to pathology for standard-of-care histologic assessment. A closed-field device is a small animal imaging platform that was repurposed for near-infrared fluorescence imaging on the back table in the operation room. This device is particularly valuable for *ex vivo* tissue specimen imaging as it has a wide dynamic range and is "closed" which allows for controlled imaging environment, including elimination of ambient light (12, 14). At pathology, the specimens were formalin-fixed and sectioned into 5-mm tissue sections. Subsequently, the tissue sections were paraffin-embedded, and a representative 5- μ m section was cut for routine hematoxylin and eosin (H&E) staining and diagnosis. On the acquired histologic H&E sections, areas with invasive or *in situ* squamous cell carcinoma were outlined by a board-certified pathologist. The slides were then digitized and analyzed for study purposes. In addition, EGFR expression of all patients was assessed through IHC of two representative tissue sections and results were scored as described previously (14).

Fluorescence intensity peak isolation and background reference

The fluorescence signal of the entire deep surface of the specimen was plotted using an interactive 3D signal-mapping plug-in (ImageJ plugin, interactive 3D surface plot) for ImageJ (version 1.50i, NIH, Washington D.C., MD). Utilizing this 3D signal-mapping tool, we were able to isolate high-intensity regions, further described as intensity peaks, from background signal (Fig. 1). By scaling of the threshold of fluorescent signal, a fluorescence signal surface map was generated from which multiple intensity peaks could be isolated. The highest intensity peaks (relative to background) were numbered, whereby the highest intensity peak (which appears first upon scaling) was assigned as the first peak, followed by the second and third peaks (Fig. 1D–G). Further isolation than the third intensity peak region was deemed unnecessary given the objective to find the closest tumor margin on the deep surface. Patients were used as their own internal control by assigning background regions located 10–15 mm from each intensity peak on the same specimen. For the statistical analysis of the fluorescence signal differences between intensity peaks and background regions on the same specimen, we quantified the signal at these regions by drawing circular (5 mm diameter) regions of interests to extract the mean fluorescence intensity (MFI) in arbitrary units (a.u.).

Correlation of fluorescence signal with margin distance

For each intensity peak and background region we measured the margin distance, which is defined as the distance in millimeters between the tumor edge and the specimen edge on the histologic sections. First, to validate our method, we evaluated whether the margin distance at the intensity peaks would be significantly less when compared with the margin distance at the background regions. Second, to evaluate whether the first intensity peak would accurately predict the closest margin, we determined whether the margin distance at the first peak would be less when compared with the second peak, and whether the margin distance at the second peak was less than the margin distance at the third peak.

To correlate the histologic sections to the appropriate intensity peaks or background regions on the deep surface, the specimens were reconstructed from the 5-mm tissue sections. This process, described by others (15), allowed us to register the margin distance measurements performed on histologic sections, to the fluorescence intensity peaks (and background regions) located on the deep surface of the specimen, within a 1–2 mm margin of error. The margin distance was measured five times on each histologic section and averaged, using ImageJ.

Statistical analysis

Per specimen, MFI [a.u.] and margin distance [mm] between the intensity peaks and background regions were compared using the Wilcoxon signed rank test. To compare MFI between the intensity peaks and background regions, the median signal intensity of the first, second, and third intensity peaks was compared with the median signal of the corresponding background regions (i.e., one/intensity peak) for each specimen. To compare margin distances for the first, second, and third intensity peak, the Wilcoxon signed rank test was used. P values of 0.05 or less were considered statistically significant. GraphPad software (Version 8.0c) was used for statistical analysis. The median is used because it is a more robust summary measure to outliers compared with the mean.

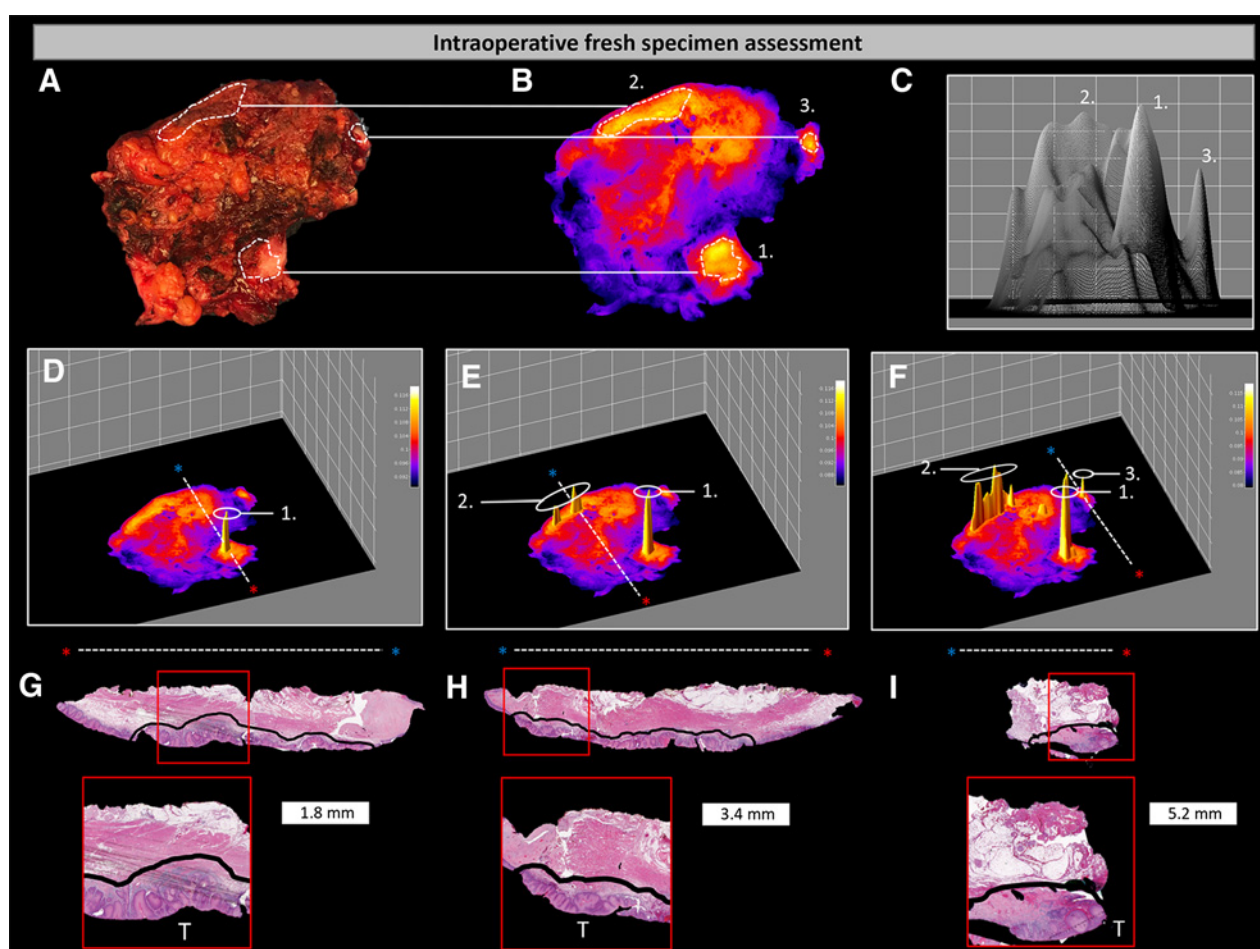


Figure 1.

Overview of workflow. Representative brightfield (**A**) and fluorescence image (**B**) of a specimen's deep margin. Number 1–3 allocate the fluorescence peaks in order of first appearance throughout the whole figure. **C**, Side view on the entire fluorescence surface map of deep margin (white arrow image **B** indicates angle). **D–F**, Identification of highest fluorescence intensity peaks on the deep surface (with color bar). The white dotted lines and asterisks (red/blue) indicate the orientation in which the H&E slides were cut. **G–I**, H&E slides with delineated tumor (black line) on which the margin distance was measured (white box). T, tumor.

Results

Patient enrollment

A total of 16 patients underwent fluorescent evaluation of their primary specimen after systemic infusion of panitumumab-IRDye800CW. Primary tumor specimens were imaged with a closed-field back table device to assess the fluorescence intensity-peaks of the deep surface. The process of imaging acquisition (30s/image) and peak-intensity isolation (120s) of a single specimen took approximately 2.5 minutes on average. Patient characteristics are summarized in Supplementary Table S1. Four patients with specimen involving bone were excluded from analysis because histologic reconstruction of the specimen could not be performed after the decalcification process. In one excluded case, shown in Supplementary Fig. S1, the intensity peak region could successfully be correlated to the corresponding H&E slide due to demarcation using a suture. For the remaining 12 patients, a total of 36 intensity peaks and 36 background regions were analyzed. Furthermore, using IHC we have identified high levels of EGFR expression in all resected tumors, as previously reported in this population (14).

Intensity peaks: higher signal, closer margin distance

First, the method was validated to determine whether intensity peaks would indeed have higher fluorescence signal and lower margin distance when compared with background regions of the same specimen. Using all specimens, the median signal for the intensity peak regions had a significantly higher MFI compared with the median signal for the background regions ($P < 0.05$, $n = 24$; Fig. 2A). Figure 2B shows the difference in margin distance of the intensity peaks compared with background regions for each patient. The overall margin distance at the intensity peaks was significantly less than the background regions in all cases ($P < 0.05$, $n = 24$).

In all specimens, the distance from margin to tumor (i.e., margin distance) was lower at the location of the first fluorescence intensity peak when compared with the second highest peak (Fig. 3). Similarly, the second highest peak intensity had a closer margin distance in 83% of samples when compared with the third highest fluorescence peak. The first fluorescence intensity peak had a significantly closer margin distance (by 2.1 mm, $P < 0.05$, $n = 24$) than the second intensity peak. In all 12 cases evaluated,

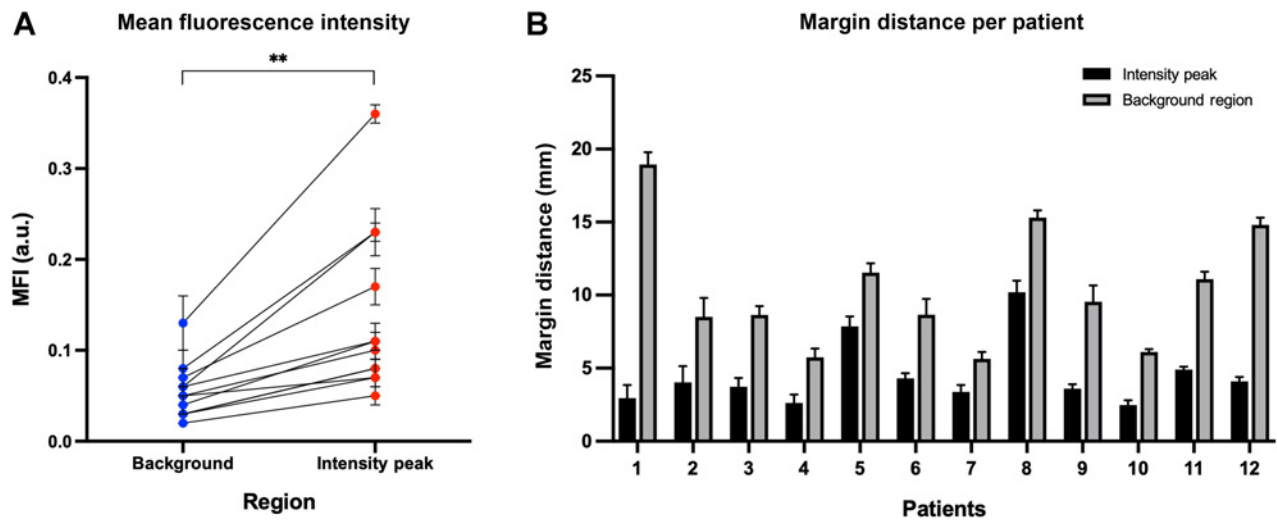


Figure 2.

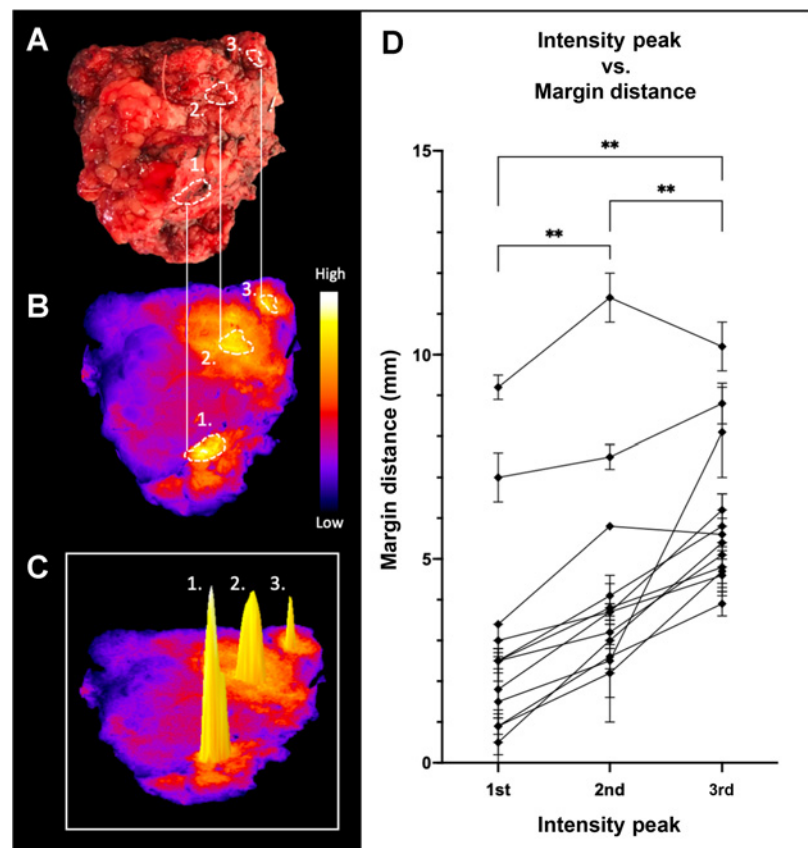
Comparison of intensity peaks versus background. **A**, First graph indicates the relative increase in MFI of all background regions to intensity peak regions per patient. **B**, The second graph illustrates the difference in margin distance for background and intensity peak regions per patient.

the first intensity peak identified the area that harbored tumor closest to the deep surface when compared with all subsequent intensity peaks ($P < 0.05$, $n = 36$). The average increase in distance between the tumor and the specimen surface was 1.6 mm when comparing the second and third intensity peaks. It is worth noting that there were two instances where the distance from the tumor to

the specimen surface did not increase between the second and third intensity peak. However, in both of these cases, the difference between the second and third intensity peak was not substantially different: the peaks were found to correlate with a margin distance that was within the margin of error (5.8 ± 0.1 mm vs. 5.6 ± 0.4 mm; and 11.4 ± 0.6 mm vs. 10.2 ± 0.6 mm).

Figure 3.

Intensity peak versus margin distance. Representative brightfield (**A**) and fluorescence image (**B**) of the deep margin (with color bar). **C**, Identification of highest fluorescence intensity peaks on the deep surface. Number 1-3 allocate the fluorescence peaks in order of first appearance. **D**, Graph showing the margin distance at the 1st, 2nd and 3rd intensity peak region per patient.



Discussion

In this study, we showed that after systemic administration of a targeted fluorescent agent, surgical specimens can be noninvasively imaged to objectively determine where tumor is located closest to the deep surface of the specimen. Because this process can be performed intraoperatively, the surgeon could use this information to immediately resect additional tissue or send a tissue sample of a suspicious region for further assessment with FSA.

Despite many advances in the field of surgical oncology, exact and reliable prediction of positive of close tumor margins remains a significant challenge, with subjective and often inaccurate use of FSA as standard-of-care. Thus, there is an important need to develop new technologies to facilitate improved intraoperative margin assessment. Here, we describe utilizing detection of a conjugated fluorescent antibody to rapidly and accurately assess intraoperative tumor margins. We have termed the margin seg-

ment with the highest fluorescence intensity as the sentinel margin—the location where the closest margin is mostly likely to be located. Analogous to sentinel lymph node assessment (where intraoperative mapping with an injected agent allows for identification of the lymph node at highest risk for metastasis), the sentinel margin may be analyzed using our described technique to identify the margin most at risk to be close or positive in a tumor specimen. This approach has significant implications in accurately and efficiently determining margin status intraoperatively.

Currently, multiple samples, sometimes upward of 15, are subjectively obtained and sent for FSA, averaging 30 minutes per sample for analysis (9, 16). The process of sentinel margin analysis takes approximately 2.5 minutes and provides an objective sampling strategy that could save a great amount of time by reducing the number of samples sent for FSA, while improving accuracy. In addition, as the process of imaging acquisition and sentinel margin analysis takes place on the back-table in parallel with the operation, it does not delay or add time to the surgery.

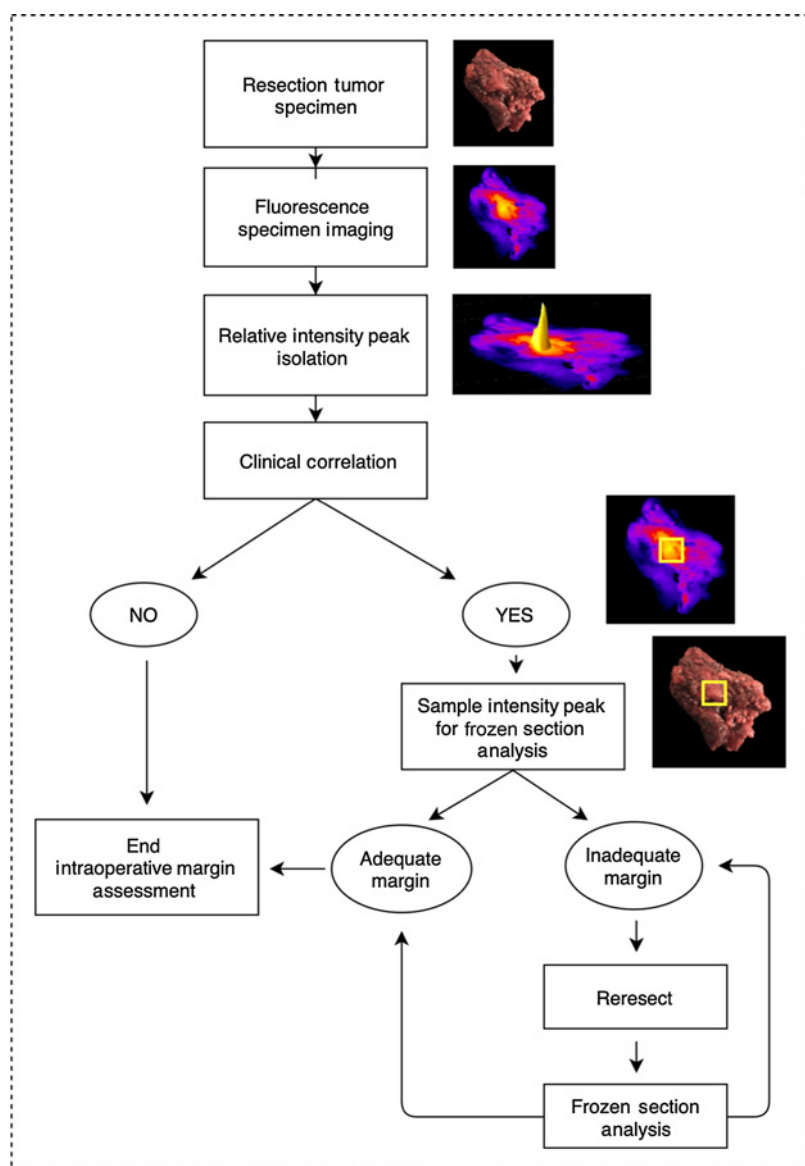


Figure 4.
Proposed workflow.

The success of this *ex vivo* specimen mapping method relies on several key optical principles. First, as a direct result of light absorption and scattering, the near-infrared signal is not detectable when it is obscured by 6 mm of tissue or more. This results in a consistently low fluorescent signal after the margin distance exceeds 5 mm, an important clinical distance in several cancer types (including head and neck cancer) as 5 mm denotes a clear margin. Historically, it has not been common to have close margins (1–5 mm) because it can be difficult to assess how much normal tissue exists between a cancer and the surgical margin. This issue can be successfully addressed utilizing this technology. Second, the optical signal intensifies as the tumor comes closer to the specimen surface. The region that has the strongest fluorescent signal (namely, the highest fluorescence intensity peak), will be easily identified at any thresholding level because the specimen fluorescence is relative to adjacent tissue of the same specimen. Ultimately, the surgeon may be able to correlate this information with clinical judgment to facilitate frozen section assessment and/or resection (17). If infiltrative tumor tissue is found closer than 5 mm to the deep surface using FSA, the surgeon has the opportunity to resect additional tissue from the wound cavity using the fluorescence intensity peaks as guidance. A clear overview of the proposed intraoperative workflow is shown in Fig. 4.

In previous studies, we have shown that fluorescence surface mapping is highly sensitive for detection of cancer within 5 mm of the surgical margin using an absolute intensity value (12, 14). However, this approach is limited as the absolute fluorescence intensity will differ between patients as a result of variance in dose and infusion-to-surgery time (14). This study, however, uses relative values, with intensity compared with background regions on the same specimen and each patient serving as his or her own internal control. Ultimately, we show that in each individual specimen we can identify the sentinel margin, and that this consistently identifies the location with the closest margin. Although we recognize that a ratio between normal and tumor tissue varies with dose, timing, and EGFR expression (14), the proposed tumor-to-tumor ratio measures relative intensity of fluorescence between different regions of the same specimen, which we hypothesize varies with the amount of overlying soft tissue (i.e., the margin distance). The data presented here provide empirical evidence that this measurement identifies the smallest (sentinel) margin of the specimen.

We have previously demonstrated that expression of EGFR, which is overexpressed in more than 90% of HNSCC, positively correlates with fluorescence intensity (14, 18). Besides the fact that fluorescence can be localized to tumor cells and varies with the level of EGFR expression, we also acknowledge that enhanced permeability and retention effect may contribute to the accumulation of panitumumab-IRDye800CW within the tumor.

Although squamous cell carcinoma is known to have a heterogeneous EGFR pattern (18, 19), overall expression appears to be high enough for successful detection of the sentinel margin in this study. It is possible however, that significant heterogeneity of EGFR expression within the tumor may influence the tumor-to-tumor ratio more than the overlying soft-tissue margin. Despite this possibility, the findings in this study suggest that sentinel margin assessment should be compatible with any fluorescent probe as well as different imaging systems as long as the probe has a similar distribution pattern as panitumumab-IRDye800CW,

and the device is capable of signal quantification and threshold scaling for isolation purposes.

Although the study included a range of tumor subsites in the head and neck region and used many data points for each specimen, the sample size limits the conclusions that can be drawn. An additional challenge is the decalcification process, although this methodology works excellent for the analysis of soft-tissue tumors, limitations presented with bone involvement will necessitate alternative research strategies.

The current standard-of-care for analysis of surgical margins remains controversial—should samples for FSA be obtained from the patient or from the specimen (20)? Our proposed strategy may help standardize specimen-driven sampling and obtaining perpendicular margins to measure tumor distance (20).

Notably, our proposed sentinel margin analysis technique can be performed in all patients undergoing tumor resection with a fluorescent contrast agent and could therefore potentially improve poor margin control in other fields where wide local excision is required, such as melanoma, colon cancer, and vulvar cancer.

Conclusion

Fluorescently labeled antibodies in combination with intraoperative fluorescence imaging can successfully identify the closest margin in head and neck cancer specimen. This technique could potentially assist intraoperative decision-making for oncologically sound resections.

Disclosure of Potential Conflicts of Interest

E. Rosenthal is a consultant/advisory board member for Vergent. No potential conflicts of interest were disclosed by the other authors.

Authors' Contributions

Conception and design: S. van Keulen, N. Nishio, B. Martin, A.D. Colevas, N.S. van den Berg, E. Rosenthal

Development of methodology: S. van Keulen, N. Nishio, A.D. Colevas, E. Rosenthal

Acquisition of data (provided animals, acquired and managed patients, provided facilities, etc.): S. van Keulen, N. Nishio, A. Birkeland, S. Fakurnejad, B. Martin, N.S. van den Berg, E. Rosenthal

Analysis and interpretation of data (e.g., statistical analysis, biostatistics, computational analysis): S. van Keulen, N. Nishio, A. Birkeland, S. Fakurnejad, K. Cunanan, A.D. Colevas, E. Rosenthal

Writing, review, and/or revision of the manuscript: S. van Keulen, N. Nishio, A. Birkeland, S. Fakurnejad, B. Martin, T. Forouzanfar, A.D. Colevas, N.S. van den Berg, E. Rosenthal

Administrative, technical, or material support (i.e., reporting or organizing data, constructing databases): S. van Keulen, N.S. van den Berg, E. Rosenthal

Study supervision: A.D. Colevas, N.S. van den Berg, E. Rosenthal

Acknowledgments

This work was supported, in part, by the Stanford Comprehensive Cancer Center, the Stanford University School of Medicine Medical Scholars Program, the Netherlands Organization for Scientific Research (Rubicon; 019.171LW.022), the NIH and the NCI (R01CA190306), and an institutional equipment loan from LI-COR Biosciences.

The costs of publication of this article were defrayed in part by the payment of page charges. This article must therefore be hereby marked *advertisement* in accordance with 18 U.S.C. Section 1734 solely to indicate this fact.

Received January 26, 2019; revised March 27, 2019; accepted May 14, 2019; published first May 29, 2019.

van Keulen et al.

References

1. Woolgar JA, Triantafyllou A. A histopathological appraisal of surgical margins in oral and oropharyngeal cancer resection specimens. *Oral Oncol* 2005;41:1034–43.
2. McMahon J, O'Brien CJ, Pathak I, Hamill R, McNeil E, Hammersley N, et al. Influence of condition of surgical margins on local recurrence and disease-specific survival in oral and oropharyngeal cancer. *Br J Oral Maxillofac Surg* 2003;41:224–31.
3. Ravasz LA, Slootweg PJ, Hordijk GJ, Smit F, van der Tweel I. The status of the resection margin as a prognostic factor in the treatment of head and neck carcinoma. *J Craniomaxillofac Surg* 1991;19:314–8.
4. Eldeeb H, Macmillan C, Elwell C, Hammod A. The effect of the surgical margins on the outcome of patients with head and neck squamous cell carcinoma: single institution experience. *Cancer Biol Med* 2012;9:29–33.
5. Cooper JS, Pajak TF, Forastiere AA, Jacobs J, Campbell BH, Saxman SB, et al. Postoperative concurrent radiotherapy and chemotherapy for high-risk squamous-cell carcinoma of the head and neck. *N Engl J Med* 2004;350:1937–44.
6. Orosco RK, Tapia VJ, Califano JA, Clary B, Cohen EEW, Kane C, et al. Positive surgical margins in the 10 most common solid cancers. *Sci Rep* 2018;8:5686.
7. Catanzaro S, Copelli C, Manfuso A, Tewfik K, Pederneschi N, Cassano L, et al. Intraoperative navigation in complex head and neck resections: indications and limits. *Int J Comput Assist Radiol Surg* 2017;12:881–7.
8. Olson SM, Hussaini M, Lewis JS Jr. Frozen section analysis of margins for head and neck tumor resections: reduction of sampling errors with a third histologic level. *Mod Pathol* 2011;24:665–70.
9. Black C, Marotti J, Zarovnya E, Paydarfar J. Critical evaluation of frozen section margins in head and neck cancer resections. *Cancer* 2006;107:2792–800.
10. Thomas Robbins K, Triantafyllou A, Suárez C, López F, Hunt JL, Strojan P, et al. Surgical margins in head and neck cancer: intra- and postoperative considerations. *Auris Nasus Larynx* 2018;46:10–7.
11. Hinni ML, Ferlito A, Brandwein-Gensler MS, Takes RP, Silver CE, Westra WH, et al. Surgical margins in head and neck cancer: a contemporary review. *Head Neck* 2013;35:1362–70.
12. van Keulen S, van den Berg NS, Nishio N, Birkeland A, Zhou Q, Lu G, et al. Rapid, non-invasive fluorescence margin assessment: optical specimen mapping in oral squamous cell carcinoma. *Oral Oncol* 2019;88:58–65.
13. Gao RW, Teraphongphom N, de Boer E, van den Berg NS, Divi V, Kaplan MJ, et al. Safety of panitumumab-IRDye800CW and cetuximab-IRDye800CW for fluorescence-guided surgical navigation in head and neck cancers. *Theranostics* 2018;8:2488–95.
14. Gao RW, Teraphongphom NT, van den Berg NS, Martin BA, Oberhelman NJ, Divi V, et al. Determination of tumor margins with surgical specimen mapping using near-infrared fluorescence. *Cancer Res* 2018;78:5144–54.
15. Lu G, Little JV, Wang X, Zhang H, Patel MR, Griffith CC, et al. Detection of head and neck cancer in surgical specimens using quantitative hyperspectral imaging. *Clin Cancer Res* 2017;23:5426–36.
16. Ord RA, Aisner S. Accuracy of frozen sections in assessing margins in oral cancer resection. *J Oral Maxillofac Surg* 1997;55:663–9.
17. van Keulen S, Nishio N, Fakurnejad S, Birkeland A, Martin BA, Lu G, et al. The clinical application of fluorescence-guided surgery in head and neck cancer. *J Nucl Med* 2019 Feb 7[Epub ahead of print].
18. Grandis JR, Melhem MF, Gooding WE, Day R, Holst VA, Wagener MM, et al. Levels of TGF- α and EGFR protein in head and neck squamous cell carcinoma and patient survival. *J Natl Cancer Inst* 1998;90:824–32.
19. Rosenthal EL, Warram JM, de Boer E, Chung TK, Korb ML, Brandwein-Gensler M, et al. Safety and tumor-specificity of cetuximab-IRDye800 for surgical navigation in head and neck cancer. *Clin Cancer Res* 2015;21:3658–66.
20. Jaafar H. Intra-operative frozen section consultation: concepts, applications and limitations. *Malays J Med Sci* 2006;13:4–12.

Clinical Cancer Research

The Sentinel Margin: Intraoperative *Ex Vivo* Specimen Mapping Using Relative Fluorescence Intensity

Stan van Keulen, Naoki Nishio, Andrew Birkeland, et al.

Clin Cancer Res 2019;25:4656-4662. Published OnlineFirst May 29, 2019.

Updated version Access the most recent version of this article at:
doi:[10.1158/1078-0432.CCR-19-0319](https://doi.org/10.1158/1078-0432.CCR-19-0319)

Supplementary Material Access the most recent supplemental material at:
<http://clincancerres.aacrjournals.org/content/suppl/2019/05/29/1078-0432.CCR-19-0319.DC1>

Cited articles This article cites 19 articles, 2 of which you can access for free at:
<http://clincancerres.aacrjournals.org/content/25/15/4656.full#ref-list-1>

E-mail alerts [Sign up to receive free email-alerts](#) related to this article or journal.

Reprints and Subscriptions To order reprints of this article or to subscribe to the journal, contact the AACR Publications Department at pubs@aacr.org.

Permissions To request permission to re-use all or part of this article, use this link
<http://clincancerres.aacrjournals.org/content/25/15/4656>.
Click on "Request Permissions" which will take you to the Copyright Clearance Center's (CCC) Rightslink site.